

# Efficient “Green” Quantum Dot-s Sensitized Solar Cells base based on Cu<sub>2</sub>S/CuInS<sub>2</sub>/ZnSe Architecture

Jia-Yaw Chang,\* Li-Fong Su, Chen-Hei Li, Chia-Chan Chang, and Jie-Mo Lin

E-mail: jychang@mail.ntust.edu.tw

Department of Chemical Engineering, National Taiwan University of Science and Technology, Taipei, Taiwan

## Experimental Section

### 1. Materials

Copper(II) nitrate hemipentahydrate (Cu(NO<sub>3</sub>)<sub>2</sub>, 98%) and selenium(IV) oxide (SeO<sub>2</sub>, 99.4%) were purchased from Alfa-Aesar (Ward Hill, USA). Indium(III) nitrate hydrate (In(NO<sub>3</sub>)<sub>3</sub>, 99.4%) and sulfur powder (S, 99.98%) was purchased from Sigma-Aldrich (Milwaukee, USA). Sodium borohydride (99.8+%), potassium chloride (99+%), sodium sulfide nonhydrate (Na<sub>2</sub>S, 98+%) was purchased from Acros Organics (New Jersey, USA), Zinc acetate dihydrate (ZnAc<sub>2</sub>, 99.8%) was obtained from J.T. Baker (Phillipsburg, USA). All organic solvents were purchased from EM Sciences. All chemicals were used directly without further purification.

### 2. Device Fabrication.

#### 2.1. Preparation of TiO<sub>2</sub> Electrodes.

Prior to the fabrication of TiO<sub>2</sub> films, fluorine-doped tin oxide (FTO) glass was ultrasonically cleaned sequentially for 30 min each in HCl, acetone, ethanol, and water. Mesoscopic TiO<sub>2</sub> films were prepared by screen printing of a TiO<sub>2</sub> slurry (Solaronix) on the FTO glass. A paste for the scattering layer containing anatase TiO<sub>2</sub> particles was deposited by screen printing, resulting in light-scattering TiO<sub>2</sub> films. This was followed by sintering at 500 °C for 30 min.

#### 2.2. Deposition of Cu<sub>2</sub>S Buffer Layer on TiO<sub>2</sub> Electrodes

To deposit Cu<sub>2</sub>S buffer layer on the TiO<sub>2</sub> electrodes, as-prepared TiO<sub>2</sub> electrodes were immersed in a solution of 1.25×10<sup>-3</sup> M Cu(NO<sub>3</sub>)<sub>2</sub> for 30 s. They were then rinsed and

immersed in a solution of 0.135 M Na<sub>2</sub>S for another 4 min, followed by another rinsing.

### 2.3. Deposition of CuInS<sub>2</sub> Sensitizer on TiO<sub>2</sub>/Cu<sub>2</sub>S Electrodes

TiO<sub>2</sub>/Cu<sub>2</sub>S electrodes prepared by the above-described procedure were successively exposed to three different solutions: one of 0.10 M In(NO<sub>3</sub>)<sub>3</sub> for 60 s, another of 1.25×10<sup>-3</sup> M Cu(NO<sub>3</sub>)<sub>2</sub> for 30 s, and a final one of 0.135 M Na<sub>2</sub>S for 4 min. After each immersion procedure, the electrode was rinsed for 1 min to remove the excess precursor solution. This SILAR process was repeated for several cycles (between two and seven) until the desired CuInS<sub>2</sub>-coated TiO<sub>2</sub> electrode was achieved. A sample that went through *n* SILAR cycles of CuInS<sub>2</sub> QD deposition is denoted as Cu<sub>2</sub>S/CuInS<sub>2</sub>(*n*).

### 2.4. Deposition of ZnS or ZnSe Passivation Layer on TiO<sub>2</sub>/CuS/CuInS<sub>2</sub>(6) Electrodes

For ZnS passivation, the TiO<sub>2</sub>/Cu<sub>2</sub>S/CuInS<sub>2</sub>(6) electrode was successively exposed for 1 min each to solutions of 0.1 M ZnAc<sub>2</sub> and 0.1 M Na<sub>2</sub>S. After each immersion procedure, the electrode was rinsed for 1 min to remove the excess precursor solution. This SILAR process was repeated several cycles until the desired ZnS passivation on the TiO<sub>2</sub>/Cu<sub>2</sub>S/CuInS<sub>2</sub> electrode was achieved. For ZnSe passivation, the TiO<sub>2</sub>/Cu<sub>2</sub>S/CuInS<sub>2</sub>(6) electrode was successively exposed for 1 min each to 0.1 M ZnAc<sub>2</sub> and a 0.1 M Se precursor solution. The Se precursor solution was prepared by heating a mixture of 0.12 M SeO<sub>2</sub> and 1.2 M NaBH<sub>4</sub> according to a modified version of a previously published procedure.<sup>1</sup> After each immersion procedure, the electrode was rinsed to remove excess precursor solution. This SILAR process was repeated for several cycles until the desired ZnSe passivation layer on the TiO<sub>2</sub>/Cu<sub>2</sub>S/CuInS<sub>2</sub>(6) electrode was achieved.

### 2.5. QD-Sensitized Solar Cell Configuration.

After preparing the QD-sensitized TiO<sub>2</sub> electrode by the SILAR process described above, the solar cells were assembled by placing a platinum-deposited conducting glass (counter electrode) prepared by thermal evaporation on the QD-sensitized TiO<sub>2</sub> electrode by using a 60-μm-thick Surlyn sheet (DuPont 1702) as a spacer. The polysulfide redox electrolyte—prepared by mixing 1.8 M Na<sub>2</sub>S, 2.0 M sulfur, and 0.2 M potassium chloride—was introduced into the sealed cell through a hole pre-drilled in the counter electrode. The active area of the cell was 0.16 cm<sup>2</sup>.

## 2.6. Sample Characterization

The field emission scanning electron microscopy (SEM) was performed on a JEOL 6335F (JEOL USA Inc., USA) equipped with an energy dispersive X-ray (EDX) analysis. The high-resolution transmission electron microscopy (TEM) images of the nanocrystals was examined by field-emission TEM on a Philips Tecnai G2 F20 microscope (Philips, Holland). Atomic force microscopy (AFM) observation was conducted using an SPM-9600 scanning probe microscope (Shimadzu Co.) at room temperature. The root mean square ( $R_{ms}$ ) was used to evaluate the surface roughness of the QD films on the basis of a  $5.0\text{ }\mu\text{m} \times 5.0\text{ }\mu\text{m}$  scan area. UV-vis–near infrared (NIR) absorption spectra were measured with a JASCO V-670 spectrometer. X-ray photoelectron spectroscopy (XPS) was performed by using a VG ESCA scientific theta probe spectrometer in constant analyzer energy mode with a pass energy of 28 eV and Al Ka (1486.6 eV) radiation as the excitation source. The photocurrent density–photovoltage characteristics of the QD-sensitized solar cell were recorded under the illumination provided by a solar simulator (Oriel 6691 450-W xenon arc lamp, CT, USA) at 100% sunlight (AM 1.5, 100 mW/cm<sup>2</sup>). A mask with a window of 0.16 cm<sup>2</sup> was clipped on the TiO<sub>2</sub> side to define the active area of the cell. The incident photon to current conversion efficiency (IPCE) plotted as a function of excitation wavelength was measured with a PEC-S20 instrument (Peccell Technologies, Inc., Kanagawa, Japan). Electrochemical impedance spectra (EIS) were measured by using an impedance analyzer (Auto Lab PGSTAT320N) at open-circuit potentials under 1 sun of illumination, with the magnitude and frequency of the alternative signal being 10 mV and  $10^{-1}$ – $10^5$  Hz, respectively.

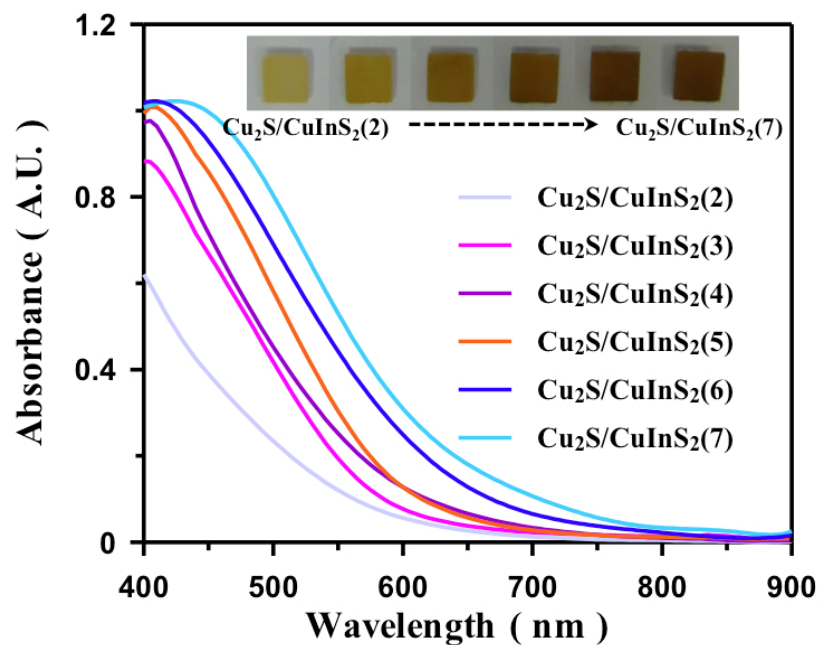


**Fig. S1.** Absorption spectra of Cu<sub>2</sub>S/CuInS<sub>2</sub> sensitized TiO<sub>2</sub> film at different numbers of CuInS<sub>2</sub> SILAR cycles. A sample after  $m$  cycles of CuInS<sub>2</sub> QD deposition is denoted as Cu<sub>2</sub>S/CuInS<sub>2</sub>( $m$ ). Inset shows a photograph of the corresponding sample deposited on TiO<sub>2</sub> film.

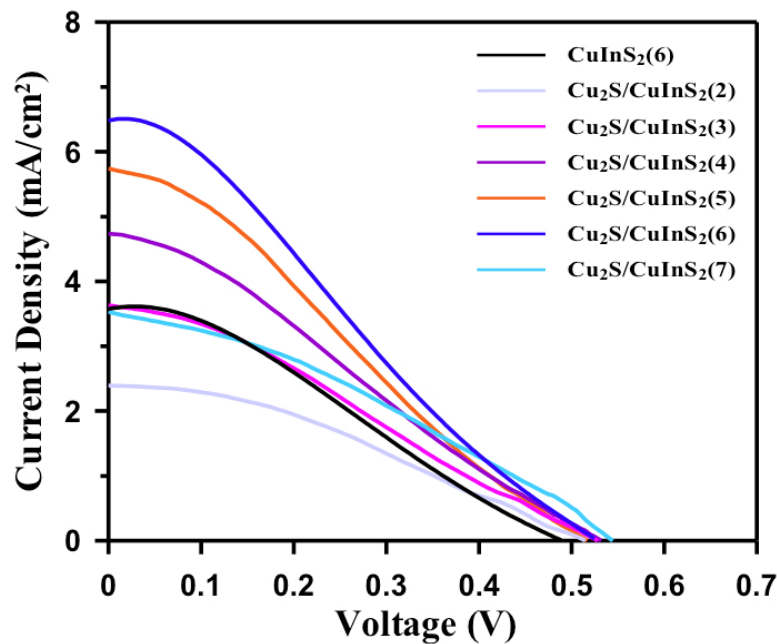


**Fig. S2.** Photocurrent density-voltage characteristic curves of QD-sensitized solar cell at different numbers of CuInS<sub>2</sub> SILAR cycles.

**Table S1.** Summary of photovoltaic properties of QD-sensitized solar cells fabricated with different sensitization conditions.

Sample	$J_{SC}$ (mA cm <sup>-2</sup> )	$V_{OC}$ (mV)	FF (%)	$\eta$ (%)
CuInS <sub>2</sub> (6)	3.65	479.8	30.3	0.53
Cu <sub>2</sub> S/CuInS <sub>2</sub> (2)	2.38	509.7	34.8	0.42
Cu <sub>2</sub> S/CuInS <sub>2</sub> (3)	3.63	524.6	29.3	0.56
Cu <sub>2</sub> S/CuInS <sub>2</sub> (4)	4.75	529.7	27.3	0.69
Cu <sub>2</sub> S/CuInS <sub>2</sub> (5)	5.74	519.9	26.9	0.80
Cu <sub>2</sub> S/CuInS <sub>2</sub> (6)	6.58	529.9	25.9	0.90
Cu <sub>2</sub> S/CuInS <sub>2</sub> (7)	3.53	544.9	32.9	0.63

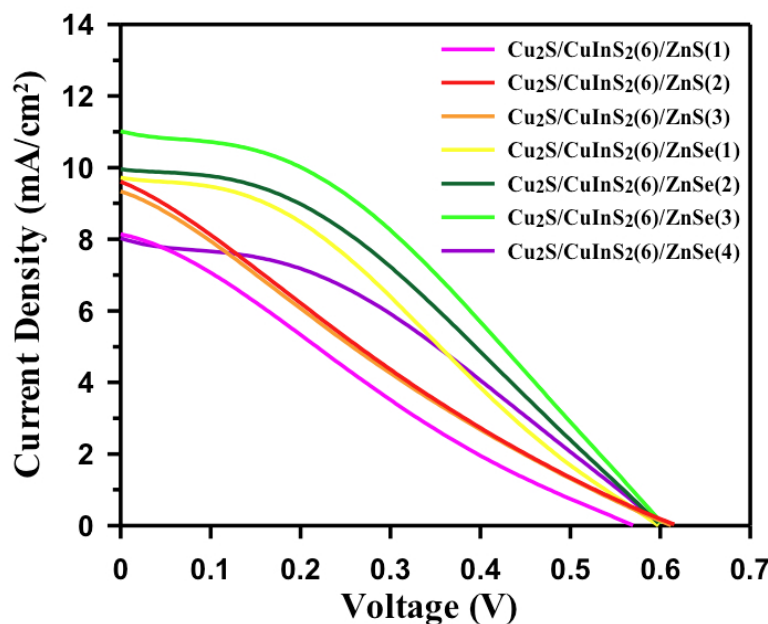


**Fig. S3.** Photocurrent density-voltage characteristic curves of  $\text{Cu}_2\text{S}/\text{CuInS}_2(6)$  QD-sensitized solar cell at different numbers of ZnS or ZnSe SILAR cycles.

**Table S2.** Summary of photovoltaic properties of the  $\text{Cu}_2\text{S}/\text{CuInS}_2(6)$  QD-sensitized solar cell at different numbers of ZnS or ZnSe SILAR cycles.

Sample	$J_{\text{SC}}$ ( $\text{mA cm}^{-2}$ )	$V_{\text{OC}}$ (mV)	FF (%)	$\eta$ (%)
$\text{Cu}_2\text{S}/\text{CuInS}_2(6)/\text{ZnS}(1)$	8.16	574.9	24.7	1.10
$\text{Cu}_2\text{S}/\text{CuInS}_2(6)/\text{ZnS}(2)$	9.62	614.9	24.1	1.33
$\text{Cu}_2\text{S}/\text{CuInS}_2(6)/\text{ZnS}(3)$	9.38	609.8	24.3	1.29
$\text{Cu}_2\text{S}/\text{CuInS}_2(6)/\text{ZnSe}(1)$	9.72	600.0	36.7	2.02
$\text{Cu}_2\text{S}/\text{CuInS}_2(6)/\text{ZnSe}(2)$	9.97	605.0	40.6	2.27
$\text{Cu}_2\text{S}/\text{CuInS}_2(6)/\text{ZnSe}(3)$	10.96	604.9	40.6	2.52
$\text{Cu}_2\text{S}/\text{CuInS}_2(6)/\text{ZnSe}(4)$	7.98	599.9	42.5	1.80

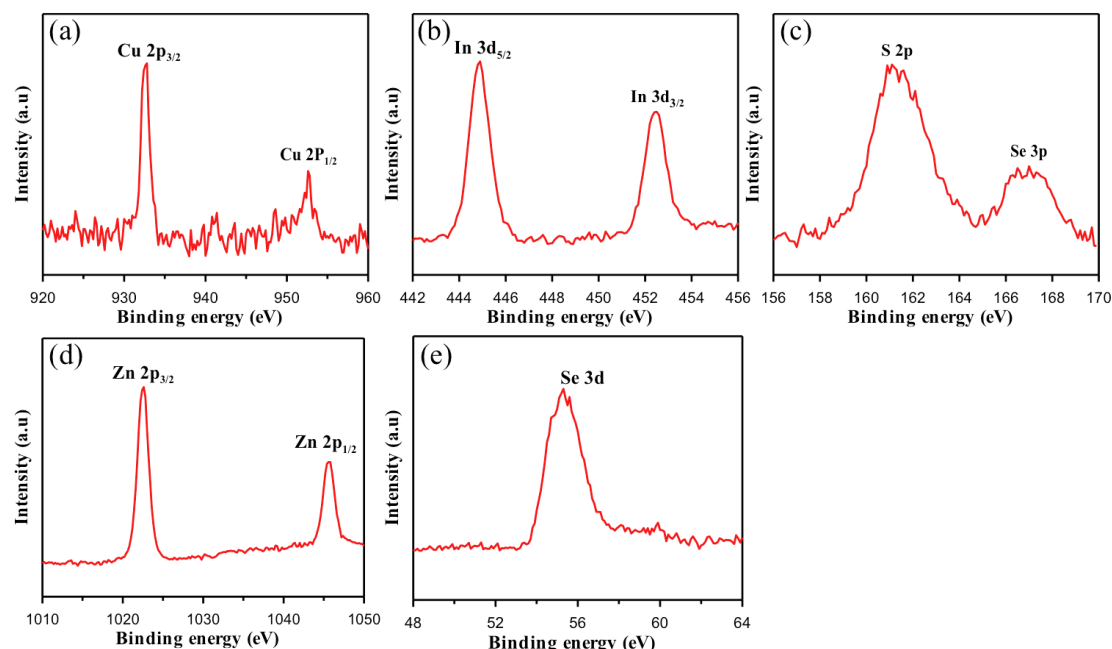


**Fig. S4.** XPS spectra of Cu<sub>2</sub>S/CuInS<sub>2</sub>/ZnSe QD-sensitized solar cell. The Cu 2p core splits into 2p<sub>3/2</sub> (932.8 eV) and 2p<sub>1/2</sub> (952.7 eV) peaks, consistent with the standard separation of 19.9 eV (Fig. S4a).<sup>2</sup> In addition, the Cu 2p<sub>3/2</sub> satellite peak of Cu(II), which is usually located at 942 eV<sup>3</sup>, does not appear in the spectrum. Therefore, it can be concluded that only monovalent copper exists in the sample. The binding energies of In 3d<sub>5/2</sub> and In 3d<sub>3/2</sub> can be assigned to 444.9 eV and 452.4 eV, respectively (Fig. S4b). The S 2p<sub>1/2</sub> peak at 161.1 eV can be assigned to the S coordinated to Cu and In (Fig. S4c). The peaks of Zn 2p appear at binding energies of 1022.6 and 1045.7 eV, which can be assigned to Zn(II) with a peak splitting of 23.1 eV<sup>4</sup> (Fig. S4d). The Se 3d peak at 55.3 eV (Fig. S4c) and the Se 3p core located at 167.0 eV (Fig. S4e), which are in good accordance with values reported previously, were assigned to Se 3p<sub>1/2</sub>.<sup>2,5</sup>

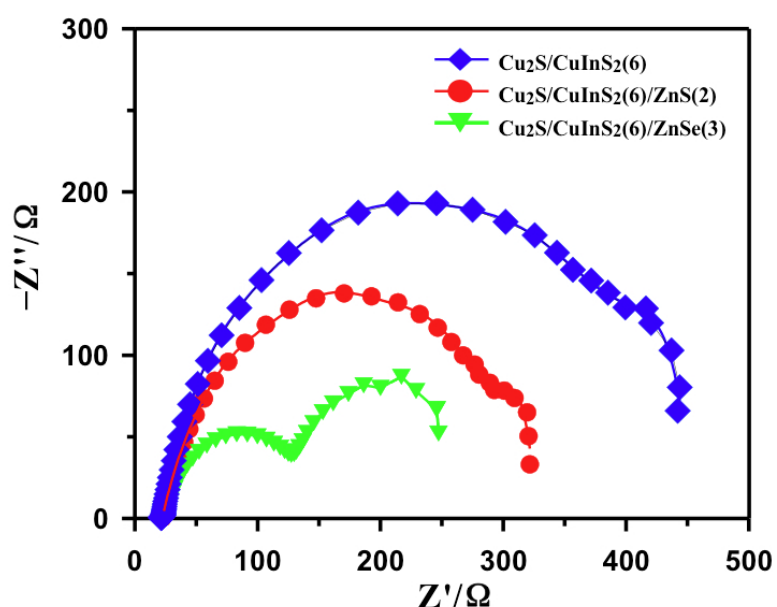


**Fig. S5.** EIS spectra of QD-sensitized solar cells fabricated with different sensitization conditions.

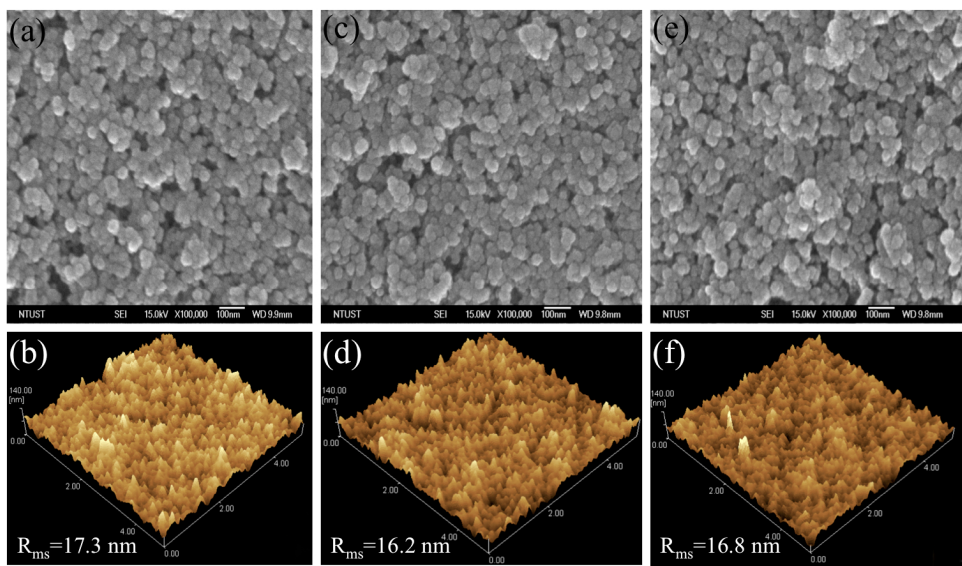


**Fig. S6.** SEM (top panels) and AFM images (bottom panels) of the (a, b)  $\text{Cu}_2\text{S}/\text{CuInS}_2(6)$ , (c, d)  $\text{Cu}_2\text{S}/\text{CuInS}_2(6)/\text{ZnS}(2)$ , and (e, f)  $\text{Cu}_2\text{S}/\text{CuInS}_2(6)/\text{ZnSe}(3)$  configurations prepared by the SILAR process.

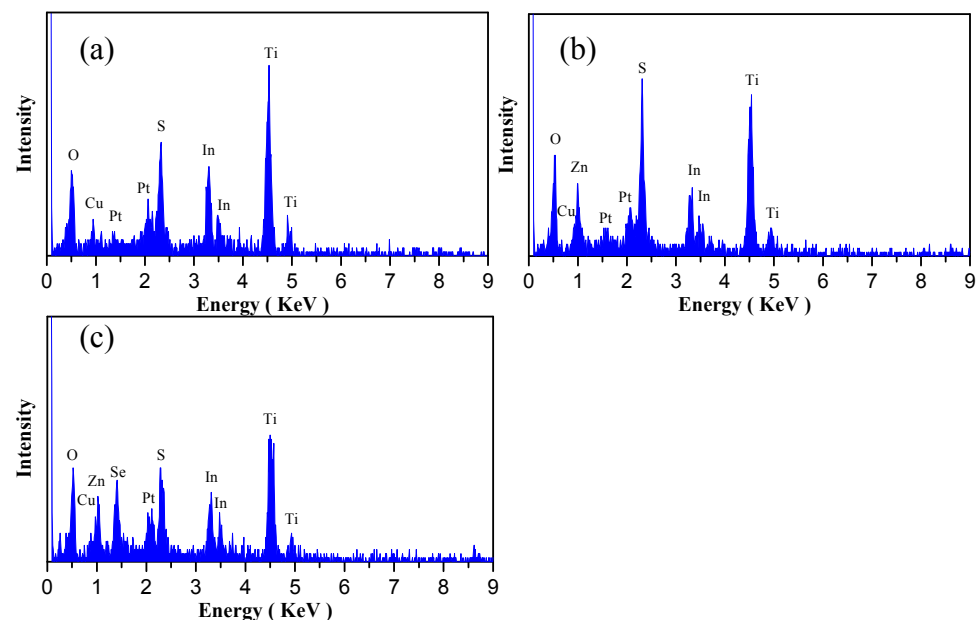


**Fig. S7.** EDX spectrum of the (a)  $\text{Cu}_2\text{S}/\text{CuInS}_2(6)$ , (b)  $\text{Cu}_2\text{S}/\text{CuInS}_2(6)/\text{ZnS}(2)$ , and (c)  $\text{Cu}_2\text{S}/\text{CuInS}_2(6)/\text{ZnSe}(3)$  configurations prepared by SILAR process. The Pt peaks are due to the sample pretreatment of SEM used in the measurement and Ti peaks come from  $\text{TiO}_2$  film.

The SEM images show that the three samples are closely packed layers composed of a network of spherical particles. However, the surface morphology variation in the  $\text{CuInS}_2$  QDs before and after deposition of a  $\text{ZnX}$  ( $\text{X}=\text{S}, \text{Se}$ ) passivation layer cannot be distinguished owing to the small size of the QDs (Fig. S6† a, c, and e).

Nonetheless, the EDX spectrum in the SEM image demonstrates that the corresponding materials were deposited on the TiO<sub>2</sub> surface, confirming the formation of CuInS<sub>2</sub> in the absence and presence of a ZnX passivation layer (Fig. S7†). AFM imaging in the tapping mode was utilized to determine the overall surface roughness. The root-mean-square roughness ( $R_{ms}$ ) represents the standard deviation of the height values within a given area and allows the surface roughness to be determined by statistical methods. It is given by<sup>6</sup>

$$R_{ms} = \sqrt{\frac{\sum_{n=1}^m (z_n - z_{av})^2}{m-1}}$$

where  $z_n$  is the current vertical distance value ( $z$ ) and  $z_{av}$  represents the average of the  $z$  values within a given area of  $m$  data points. The AFM image of Cu<sub>2</sub>S/CuInS<sub>2</sub>(6) QDs on the surface of the TiO<sub>2</sub> film in Fig. S6† shows a granular homogeneous morphology with a  $R_{ms}$  roughness of 17.3 nm. The images in Fig. S6†d and f, obtained from the Cu<sub>2</sub>S/CuInS<sub>2</sub> QD film with ZnS or ZnSe passivation layers, revealed a relatively smooth surface for both thin films and the  $R_{ms}$  roughness of the surface decreased to 16.2 and 16.8 nm for the ZnS and ZnSe passivation layer, respectively. Clearly, the surface quality of Cu<sub>2</sub>S/CuInS<sub>2</sub> thin films could be greatly improved by deposition of a ZnS or ZnSe passivation layer.

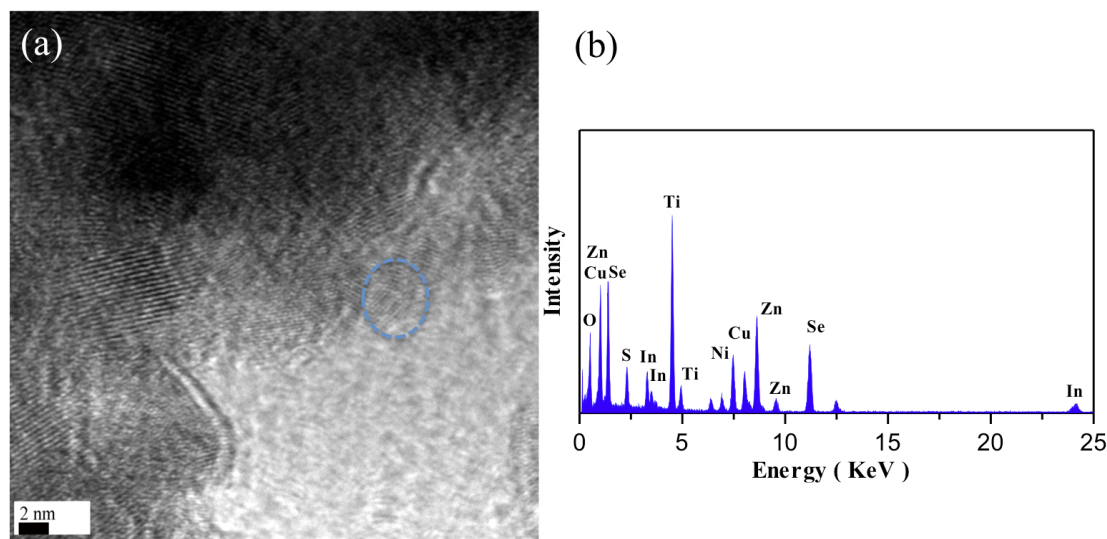


**Fig. S8.** (a) TEM images of  $\text{Cu}_2\text{S}/\text{CuInS}_2(6)/\text{ZnSe}(3)$  configurations prepared by SILAR process. Blue square dots represent the QDs deopised on the  $\text{TiO}_2$  nanocrystals (b) EDX spectrum of  $\text{Cu}_2\text{S}/\text{CuInS}_2(6)/\text{ZnSe}(3)$  deopised on the  $\text{TiO}_2$  nanocrystals. The Ni peaks are due to the Ni TEM grid used in the measurement.

## Referneces

1. H. Lee, M. Wang, P. Chan, D. R. Gamelin, S. M. Zakeeruddin, M. Gratzel and M. K. Nazeeruddin, *Nano Lett.*, 2009, **9**, 4221.
2. S. Li, Z. Zhao, Q. Liu, L. Huang, G. Wang, D. Pan, H. Zhang and X. He, *Inorg. Chem.*, 2011, **50**, 11958.
3. L. D. Partain, R. A. Schneider, L. F. Donaghey, P. S. Mcleod, *J. Appl. Phys.*, 1985, **57**, 5056.
4. Q. Guo, S. J. Kim, M. Kar, W. N. Shafarman, R. W. Birkmire, E. A. Stach, R. Agrawal and H. W. Hillhouse, *Nano Lett.*, 2008, **8**, 2982.
5. M. -Y. Chiang, S -H. Chang, C. -Y. Chen, F. -W. Yuan and H. -Y. Tuan, *J. Phys. Chem. C.*, 2011, **115**, 1592.
6. P. Cacciafesta, K. R. Hallam, A. C. Watkinson, G. C. Allen, M. J. Miles and K. D. Jandt, *Surf. Sci.*, 2001, **491**, 405.